Available online at www.sciencedirect.com
SCIENCE DIRECT®
Biochemical and Biophysical Research Communications 300 (2003) 271–277
BBRC
www.elsevier.com/locate/ybbrc

Structures of cadmium-binding acidic phospholipase A_2 from the venom of *Agkistrodon halys* Pallas at 1.9 Å resolution

Sujuan Xu,[a] Lichuan Gu,[a] Tao Jiang,[a] Yuancong Zhou,[b] and Zhengjiong Lin[a,*]

[a] *National Laboratory of Biomacromolecules, Institute of Biophysics, Chinese Academy of Sciences, Beijing 100101, China*
[b] *Key Laboratory of Proteomics, Institute of Biochemistry and Cell Biology, Shanghai Institutes for Biological Sciences, Chinese Academy of Sciences, Shanghai 200031, China*

Received 15 November 2002

Abstract

Phospholipase A_2 coordinates Ca^{2+} ion through three carbonyl oxygen atoms of residues 28, 30, and 32, two carboxyl oxygen atoms of residue Asp49, and two (or one) water molecules, forming seven (or six) coordinate geometry of Ca^{2+} ligands. Two crystal structures of cadmium-binding acidic phospholipase A_2 from the venom of *Agkistrodon halys* Pallas (i.e., *Agkistrodon blomhoffii* brevicaudus) at different pH values (5.9 and 7.4) were determined to 1.9 Å resolution by the isomorphous difference Fourier method. The well-refined structures revealed that a Cd^{2+} ion occupied the position expected for a Ca^{2+} ion, and that the substitution of Cd^{2+} for Ca^{2+} resulted in detectable changes in the metal-binding region: one of the carboxyl oxygen atoms from residue Asp49 was farther from the metal ion while the other one was closer and there were no water molecules coordinating to the metal ion. Thus the Cd^{2+}-binding region appears to have four coordinating oxygen ligands. The cadmium binding to the enzyme induced no other significant conformational change in the enzyme molecule elsewhere. The mechanism for divalent cadmium cation to support substrate binding but not catalysis is discussed.

Keywords: Phospholipase A_2; Crystal structure; Cadmium-binding region

Phospholipase A_2 (PLA_2s, EC 3.1.1.4) catalyzes the hydrolysis of the fatty acid ester at the *sn*-2 position of phospholipids with Ca^{2+} as an obligatory cofactor. It is one of the most important enzymes for the metabolism of lipids. In addition to being a catalyst for the hydrolysis of phospholipids, PLA_2 from snake venom exhibits a wide variety of pharmacological activities such as neurotoxicity, hemolytic activity, myotoxicity, and anticoagulation and antiplatelet activities [1].

The venom of *Agkistrodon halys* Pallas (*A. h.* Pallas) contains three homologous PLA_2s, which belong to group II secreted PLA_2. *A. h.* Pallas acidic PLA_2 ($APLA_2$) shows weaker toxicity and higher enzymatic activity than the other two PLA_2s [2] and can inhibit platelet aggregation. Its Ca^{2+}-binding structure has been determined at 2 and 1.6 Å resolution [3,4].

Ca^{2+} is an obligatory cofactor for catalysis by secreted PLA_2 [5,6]. As a part of the highly conserved active site, Ca^{2+} is present in a pentagonal bipyramidal (or pentagonal monopyramidal) coordination shell formed by seven (or six) oxygen ligands [3,7–9]. Two (or one) oxygen ligands are from water molecules and one of them plays the role of nucleophile in the chemical step of the catalytic cycle of PLA_2 [9–11]. The catalytic significance of several divalent cations for secreted phospholipase A_2 was reported. Ca^{2+} is essential both for substrate binding and for catalysis, while Cd^{2+} supports substrate binding but not catalysis [12,13].

This paper reports the 1.9 Å resolution crystal structures of Cd^{2+}-binding *A. h.* Pallas $APLA_2$ and discusses the mechanism for Cd^{2+} to support substrate binding but not catalysis of the substrate based on these structural data.

Materials and methods

Protein purification and measurement of phospholipase activity. Acidic PLA_2 was isolated and purified from the venom of *A. halys*

* Corresponding author. Fax: +86-10-6487-1293.
E-mail address: lin@sun5.ibp.ac.cn (Z. Lin).

0006-291X/02/$ - see front matter © 2002 Elsevier Science (USA). All rights reserved.
PII: S0006-291X(02)02833-4

Pallas (i.e., *Agkistrodon blomhoffii* brevicaudus) according to the method reported previously [14]. Phospholipase activity was measured using pH-stat method at room temperature [15].

Crystallization and data collection. Crystallization trials were performed by the hanging drop vapor-diffusion method at 291 K. Crystals suitable for X-ray analysis were obtained at pH 5.9 and 7.4. The optimal crystallization conditions for growing crystals suitable for X-ray analysis were as follows: a droplet containing 10 mg ml^{-1} protein, 10% (v/v) 1,4-butyldiol, 0.01 M $CdCl_2$, and 0.1 M $Na(CH_3)_2AsO$ as buffer (pH = 7.4 or 5.9) was equilibrated over a reservoir solution containing 60% (v/v) 1,4-butyldiol. Crystals grown at pH 7.4 were designated as crystal-I and crystals grown at pH 5.9 were designated as crystal-II. Diffraction data were collected on a Mar 345 Research Image Plate detector mounted on a Rigaku rotating Cu anode X-ray generator operating at 40 kV and 50 mA ($\lambda = 1.5418$ Å). A total of 120 frames for crystal-I and 168 frames for crystal-II with an oscillation angle of 1° and an exposure time of 600 s per frame were measured with the crystal-detector distance set to 130 mm.The data were processed using HKL Suite program [16]. The final merged data sets had an *R*-merge of 6.8% and completeness of 99.9% for crystal-I and *R*-merge of 7.5% and completeness of 99.9% for crystal-II between 25 and 1.9 Å. Both data sets showed high redundancies and average $I/\sigma(I)$. Details of the data-collection statistics are summarized in Table 1.

Structure determination and refinement. As both of the crystals were isomorphous with Ca^{2+}-binding *A. h.* Pallas $APLA_2$, their structures were determined by the isomorphous difference Fourier method with Ca^{2+}-binding *A. h.* Pallas $APLA_2$ (entry 1PSJ in Brookhaven Protein Data Bank) as an initial model. The refinement was carried out using the CNS program [17] with 10% of the data reserved to calculate the free *R* factor [18]. Both structures were refined in the resolution range of 25–1.9 Å using 10,434 reflections and 10,417 reflections. Model rebuilding was carried out with the Turbo/Frodo graphics program on an O2 workstation. Atomic models were iteratively adjusted according to the $2F_o$–F_c and F_o–F_c electron density maps. During the refinement, the side-chain of the residue Leu112 in the initial model was found to be inconsistent with its electron density and environment and this residue was then reassigned as Thr112. Reassignment of residue 112 as threonine is supported by the reported amino acid sequence of *A. h.* Pallas acidic PLA_2 induced from cDNA [19]. In this experiment, cadmium cations (0.01 M) instead of calcium cations were added into the crystallization solutions, and the competition experiment implies that cadmium cations may occupy the position of calcium cations in the Ca^{2+}-binding loop (data not shown). Thus a high electron density peak located at the center of the Ca^{2+}-binding loop was considered as a cadmium cation and included in the model. No other site for binding Cd^{2+} was found. Finally, 1,4-butyl glycol molecules and water molecules were included in the model based on their electron densities and environments. After several cycles of atomic position and group *B*-factor refinements and model rebuilding, the *R* values and *R*-free values of the two structures converged with the F_o–F_c map, showing no more obvious uninterpretable features.

Results

Model quality

Each of the final models consisted of 954 non-H protein atoms, a cadmium cation, two 1,4-butyl glycol molecules, and water molecules (81 for crystal-I and 112 for crystal-II). The final models had good stereochemistry and acceptable rms deviations from ideal values for bond lengths and bond angles. Calculations of the two models by the PROCHECK program [20] indicated that 93.3% non-glycine residues in the asymmetric unit were located in the most favored regions and the remaining 6.7% were in the additional allowed regions. The two crystal structures had continuous and well-defined corresponding $2F_o$–F_c electron density for both the backbone and the side-chains except for a very few polar side-chains on the molecule surface. The crystallographic *R* and *R*-free values of both structures were between 18.8% and

Table 1
Diffraction data-collection statistics and refinement results

	Crystal-I	Crystal-II
Space group	$P6_1$	$P6_1$
Cell parameters	$a = b = 83.27$ Å, $c = 32.80$ Å, $\alpha = \beta = 90°$, $\gamma = 120°$	$a = b = 83.16$ Å, $c = 32.78$ Å, $\alpha = \beta = 90°$, $\gamma = 120°$
Resolution range (Å)	25–1.9	25–1.9
R_{merge} (%)	6.8 (36.9)	7.2 (26.0)
Completeness of data (%)	99.9 (100)	100 (100)
Average $I/\sigma(I)$	26.2 (5.7)	33.7 (9.7)
Total of observations	128,952	187,637
Total of unique reflections	10,454	10,431
No. of mols/asym. unit	1	1
Crystallographic *R* factor (%)	18.8	19.8
Crystallographic *R*-free factor (%)	19.9	20.8
No. of non-H protein atoms	904	904
No. of solvent molecules		
Water	81	112
1,4-butyl glycol	2	2
Rms deviations from ideality		
Bond distances (Å)	0.007	0.006
Bond angles (°)	1.31	1.23
Dihedral angles (°)	22.59	22.64
Improper angles (°)	0.83	0.82

Values in parentheses are for the highest solution shell (1.97–1.90 Å).

20.8%, indicating the high quality of the two structure models. The refinement results are listed in Table 1. The coordinates for both structures have been deposited in the Protein Data Bank (PDB codes: 1M8R & 1M8S).

Description of the structures

Structures for crystal-I and crystal-II are nearly identical to each other; the Cα rms deviation between the two structures is only 0.04 Å. The general structural features of Cd^{2+}-binding *A. h.* Pallas $APLA_2$ are shown in Fig. 1. These features are extremely similar to those of previously established Ca^{2+}-binding *A. h.* Pallas $APLA_2$ [3,4]. Superposition of the Cα atom positions of the Cd^{2+}-binding and Ca^{2+}-binding $APLA_2$ structures showed a Cα rms deviation of less than 0.14 Å. The similarity includes the active site, the hydrophobic channel, and most of the water molecules (65 water molecules were common to all; among them 21 formed two or more hydrogen bonds with the protein molecule).

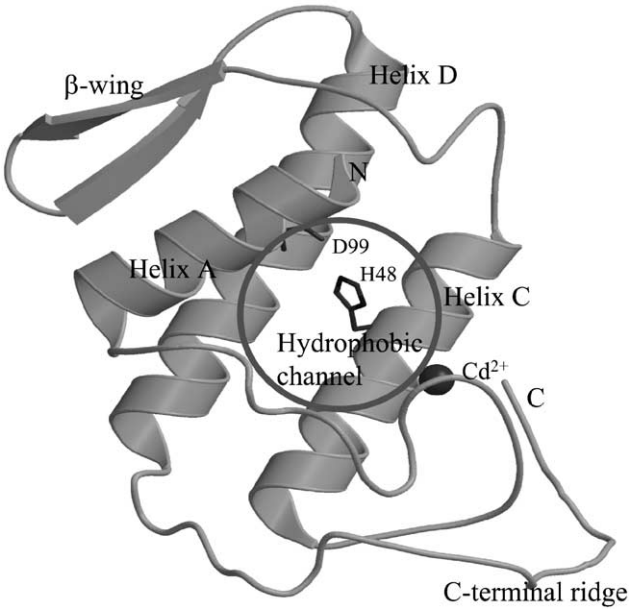

Fig. 1. The Cα backbone structure of Cd^{2+}-binding *A. h.* Pallas $APLA_2$. The structure consists of three long α-helices (αA, αC, and αD) and one double-stranded antiparallel β-sheet designated as β-wing. *Note*. Programs Molscript [32] and Raster3D [33] were used for drawing this figure. Figs. 1–5 were prepared using the data from crystal-I.

Both structures revealed pentagonal water rings formed by hydrogen bonds. The rings are located near residues Cys44 and Cys98 and are hydrogen bonded to their carbonyl oxygen atoms (Fig. 2). The ring structure has an average hydrogen bond distance of 3.03 Å and apex angles from 102° to 111°. This water ring was not observed in the Ca^{2+}-binding $APLA_2$ structures [3,4]. Pentagon rings of water molecules have abundant hydrogen bonds and have been reported in other high-resolution protein structures [21].

Both structures showed reasonable stereochemistry around the reassigned residue 112 (Fig. 3). The oxygen atom from the side-chain of Thr112 formed two hydrogen bonds with water molecules W6 and W30. W6 was subsequently hydrogen bonded to Asp39OD1, Thr41OG1, and Thr41N and W30 to Asn111ND2 and Asn109OD1. These water bridges stabilize a region near N-term of helix αC and C-term of helix αD.

The most significant difference between the Cd^{2+}-binding and Ca^{2+}-binding *A. h.* Pallas $APLA_2$ occurred in the metal-binding region, which is described in the following section.

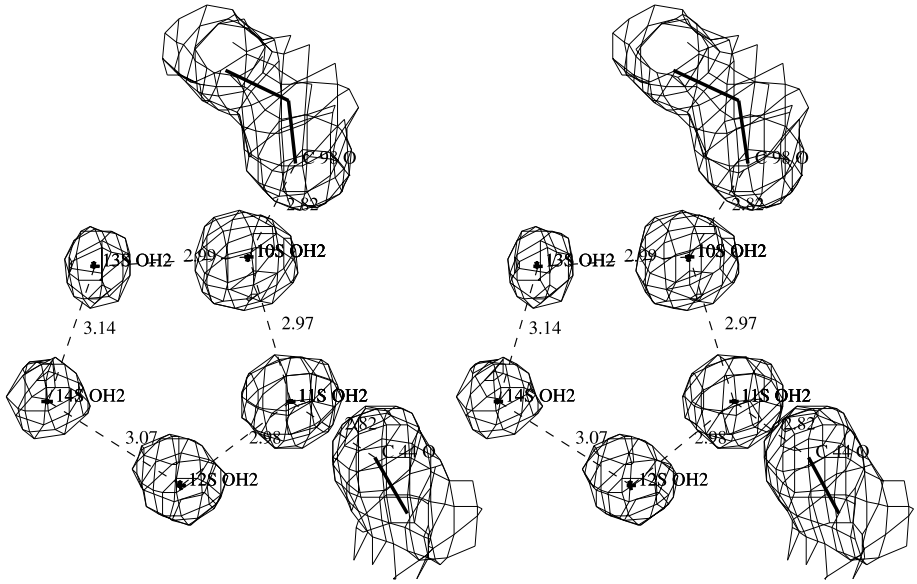

Fig. 2. Stereo view of the pentagonal water structure.

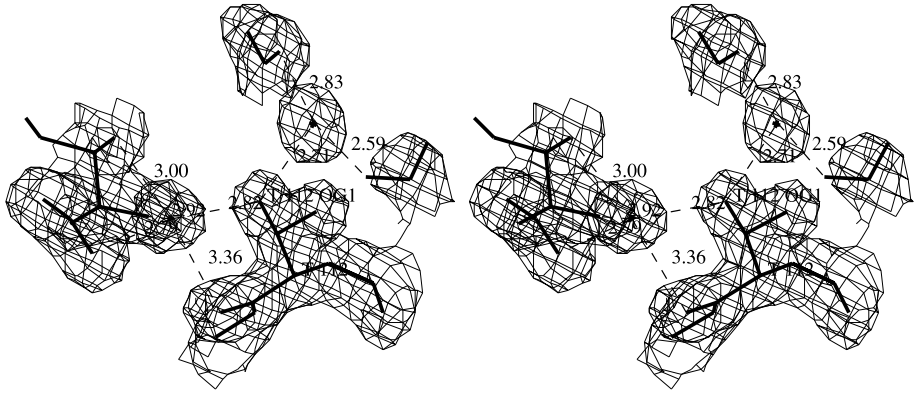

Fig. 3. Stereo view of the $2F_o$–F_c omit map around the residue Thr112.

Cd^{2+} and its ligands

Conformation of the Ca^{2+}-binding region in the structures of Ca^{2+}-binding PLA_2 reported previously is conservative, in which calcium cation is coordinated to seven (or six) oxygen ligands [22]: three from backbone carbonyls of highly conserved residues Tyr28, Gly30, and Gly32, two from the carboxyl group of Asp49, and two (or one) from water molecules. The seven (or six) ligands form a pentagonal bipyramidal (or pentagonal monopyramidal) conformation. The Ca^{2+}-binding *A. h.* Pallas $APLA_2$ shares the same Ca^{2+}-binding region

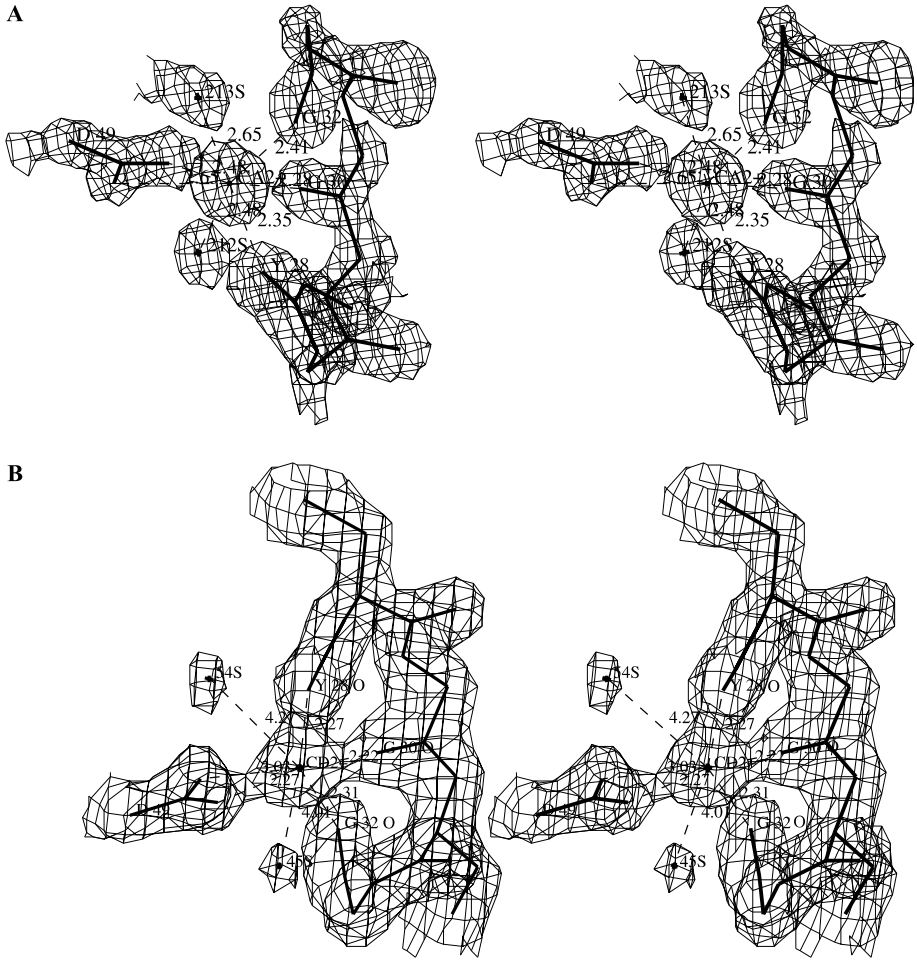

Fig. 4. (A) Stereo view of the $2F_o$–F_c map of Ca^{2+} and its coordination ligands in the structure of Ca^{2+}-binding *A. h.* Pallas $APLA_2$. (B) Stereo view of the $2F_o$–F_c map of Cd^{2+} and its coordination ligands in the structure of Cd^{2+}-binding *A. h.* Pallas $APLA_2$.

Table 2
Distances between cation and the coordination ligands (Å)

	Crystal-I	Crystal-II	AAA	1PSJ	1POA	1G4I	4BP2
28 O	2.27	2.31	2.35	2.27	2.33	2.35	2.45
30 O	2.22	2.27	2.27	2.24	2.46	2.31–2.47	2.56
32 O	2.31	2.32	2.40	2.28	2.18	2.32–2.36	2.40
49 OD2	2.27	2.23	2.49	2.50	2.35	2.47	2.45
49 OD1	(3.03)	(2.90)	2.66	2.80	2.56	2.50	2.54
H_2O-I			2.47	2.78	2.51	2.41	2.56
H_2O-II			2.66	(3.20)	2.44		2.40

AAA, Ca^{2+}-binding *A. h.* Pallas $APLA_2$ (1.6 Å, [4]); 1PSJ, Ca^{2+}-binding *A. h.* Pallas $APLA_2$ (2.0 Å, [3]); 1POA, *Naja naja* atra PLA_2 [29]; 1G4I, bovine pancreatic PLA_2 [30]; 4BP2, bovine pancreatic PLA_2 [31].

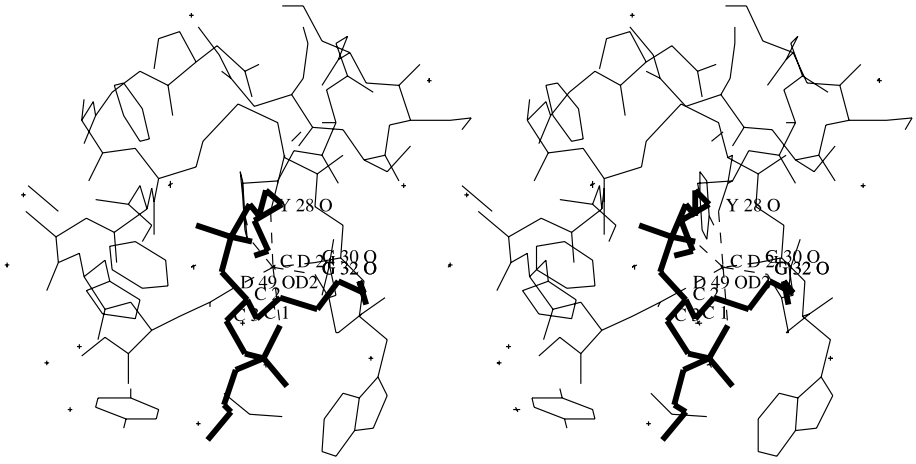

Fig. 5. Stereo view of the model of Cd^{2+}-binding *A. h.* Pallas $APLA_2$ complexed with the phosphonate transition-state analogue.

feature of PLA_2 [3,4] as shown clearly in Fig. 4A. Compared with Ca^{2+}-binding *A. h.* Pallas $APLA_2$, the side-chain of Asp49 of Cd^{2+}-binding *A. h.* Pallas $APLA_2$ shows conformational changes, which results in one oxygen atom of the carboxyl group being farther away from the cation and the other oxygen atom being nearer to the cation. The distances between the cation and the two oxygen atoms from the carboxyl group of Asp49 are 2.27 and 3.03 Å in crystal-I (2.23 and 2.90 Å in crystal-II), so only one oxygen atom from the carboxyl group of Asp49 coordinates to the cation. In addition, there is no water molecule coordinating to the cation. As a result, only four oxygen ligands coordinate to Cd^{2+}: three from backbone carbonyls of residues Tyr28, Gly30, and Gly32, one from the carboxyl group of Asp49, forming a distorted tetrahedron (Fig. 4B). The average distance between Cd^{2+} and its ligand oxygen atom is 2.27 Å, less than that of Ca^{2+}, 2.40 Å [23]. Such four-coordinate geometry of Cd^{2+} ligands is distinguished from the seven- (or six-) coordinate geometry of Ca^{2+} ligands in Ca^{2+}-binding PLA_2 structures. Table 2 lists the metal–oxygen distances in the Cd^{2+}-binding site and the Ca^{2+}-binding site of *A. h.* Pallas $APLA_2$. The high-resolution structures of Ca^{2+}-binding PLA_2 from *Naja naja* atra PLA_2 and bovine pancreatic PLA_2 are also listed for a comparison.The substitution of Cd^{2+} for Ca^{2+} induced no other significant conformational change in the enzyme molecule elsewhere.

Discussion

The structures of Cd^{2+}-$APLA_2$ crystals grown at pH of 5.9 and 7.4 are nearly identical to each other (Cα rms deviation: 0.04 Å). Thus, the effect of the variation of crystallization pH value on the structure is negligible.

Calcium cation (II) is essential both for substrate binding and for catalysis, while cadmium cation (II) supports substrate binding but not catalysis [11–13]. This study measured the phospholipase activity of *A. h.* Pallas $APLA_2$ in the presence of both calcium cation (II) and cadmium cation (II), and found that the phospholipase activity decreased with the increase of the cadmium cation (II) concentration, but increased with the increase of the calcium cation (II) concentration (data not shown). The results of the study showed that cadmium cation (II) inhibited phospholipase activity by competing with calcium cation (II), and it is very likely that cadmium cation binds to the calcium-binding loop of *A. h.* Pallas $APLA_2$.

The present Cd^{2+}-binding $APLA_2$ structures show that the cadmium cation binds to the active site as expected, and Cd^{2+} coordinates to four oxygen atoms, forming distorted tetrahedron ligands. It has been predicted by Yu et al. [11] that the four-coordinate geometry of Cd^{2+} could be achieved if the carboxylate of Asp49 provides a single ligand. Geometrical considerations suggest that coordination numbers from 4 to 6 are possible without a change in the position and geometry of the four oxygen ligands provided by the protein. Therefore the possible mechanism for Cd^{2+} to support the binding of substrate is as follows: two oxygen atoms from sn-2-carbonyl and sn-3-phosphoester groups of the substrate may coordinate to Cd^{2+} and then the coordination number of Cd^{2+} expands from 4 to 6 and the ligands form a distorted octahedral symmetry. A model-building study using the phosphonate transition-state analogue of PLA_2 from the complex structure of *Naja naja* atra PLA_2 [24] as a substrate shows that the substrate analogue fits well with the enzyme without close contacts, and the ligands coordinating to cadmium cation exhibit reasonable octahedral symmetry (Fig. 5). The fact that Cd^{2+} can exhibit different coordination numbers from 4 to 6 and different geometries in the structures of Cd^{2+}-binding protein supports this viewpoint [25–28]. Water molecules coordinating to Ca^{2+} in the structure of Ca^{2+}-binding $APLA_2$ disappeared from the structure of Cd^{2+}-binding $APLA_2$. As one of the water molecules in the coordination sphere of the cation plays the role of a nucleophile in the catalytic mechanism [9–11], the disappearance of the water molecules may be the reason for Cd^{2+} not to support the hydrolysis of the substrate.

Acknowledgments

This work was supported by the Science Fund of the Chinese Academy of Sciences. We thank Mr. Xudong Zhao for his help during data collection and processing.

References

[1] R.M. Kini, Phospholipase A_2—a complex multifunctional protein puzzle, in: R.M. Kini (Ed.), Venom Phospholipase A_2 Enzymes: Structure, Function and Mechanism, John Wiley, New York, 1997, pp. 1–28.

[2] Y.C. Chen, J.M. Maraganore, I. Reardon, R. Heinrikson, Characterization of the structure and function of three phospholipase A_2 from the venom of *Agkistrodon halys* Pallas, Toxicon 25 (1987) 401–409.

[3] X.Q. Wang, J. Yang, L.L. Gui, Z.J. Lin, Y.C. Chen, Y.C. Zhou, Crystal structure of an acidic phospholipase A_2 from the venom of *Agkistrodon halys* Pallas at 2.0 Å resolution, J. Mol. Biol. 255 (1996) 669–676.

[4] X.Q. Wang, H.Y. Zhao, Z.J. Lin, Y.C. Zhou, Crystal structure of Ca^{2+} ion saturated acidic phospholipase A_2 from *Agkistrodon halys* Pallas, Acta Biochim. Biophy. Sinica 29 (1997) 142–149.

[5] G.H. de Haas, P.P.M. Bonsen, W.A. Pieteson, L.L.M. van Deenen, Studies on phospholipase A and its zymogen from porcine pancreas: III. Action of the enzyme on short-chain lecithins, Biochim. Biophys. Acta 239 (1971) 252–266.

[6] H.M. Verheij, J.J. Volwerk, E.H.J.M. Jansen, W.C. Puyk, B.W. Dijkstra, J. Drenth, G.H. de Haas, Methylation of histidine-48 in pancreatic phospholipase A_2. Role of histidine and calcium ion in the catalytic mechanism, Biochemistry 19 (1980) 743–750.

[7] B.W. Dijkstra, J. Drenth, K.H. Kalk, Active site and catalytic mechanism of phospholipase A_2, Nature 289 (1981) 604–606.

[8] D.L. Scott, A.M. Mandel, P.B. Sigler, B. Honig, The electrostatic basis for the interfacial binding of secretary phospholipases A_2, Biophys. J. 67 (1994) 493–504.

[9] K. Sekar, S. Eswaramoorthy, M.K. Jain, M. Sundaralingam, Crystal structure of the complex of bovine pancreatic phospholipase A_2 with the inhibitor 1-hexadecyl-3-(trifluoroethyl)-sn-glycero-2-phosphomethanol, Biochemistry 36 (1997) 14186–14191.

[10] J. Rogers, B.Z. Yu, S.V. Serves, G.M. Tsivgoulis, D.N. Sotiropoulos, P.V. Ioannou, M.K. Jain, Kinetic basis for the substrate specificity during hydrolysis of phospholipids by secreted phospholipase A_2, Biochemistry 35 (1996) 9375–9384.

[11] B.Z. Yu, J. Rogers, R.N. Gordon, K.H. Theopold, K. Seshadri, S. Vishweshwara, M.K. Jain, Catalytic significance of the specificity of divalent cations as Ks* and Kcat* cofactors for secreted phospholipase A_2, Biochemistry 37 (1998) 12576–12587.

[12] T.C. Tsai, J. Hart, R.T. Jiang, K. Bruzik, M.D. Tsai, Phospholipids chiral at phosphorus. Use of chiral thiophosphatidylcholine to study the metal-binding properties of bee venom phospholipase A_2, Biochemistry 24 (1985) 3180–3188.

[13] B.Z. Yu, O.G. Berg, M.K. Jain, The divalent cation is obligatory for the binding of ligands to the catalytic site of secreted phospholipase A_2, Biochemistry 32 (1993) 6485–6492.

[14] X.F. Wu, Z.P. Jiang, Y.C. Chen, A comparison of three phospholipase from the venom of *Agkistrodon halys* Pallas, Acta Biochim. Biophy. Sinica 16 (1984) 664–671.

[15] X. Zhang, L. Zheng, N.Q. Lin, K.C. Ruan, Y.C. Zhou, Effect of calcium ion on the structure and function of phospholipase A2 from the venom of *Agkistrodon halys* Pallas, Chin. Biochem. J. 10 (1994) 330–334.

[16] Z. Otwinowski, W. Minor, Processing of X-ray diffraction data collected in oscillation mode, Methods Enzymol. 276 (1997) 307–326.

[17] A.T. Brunger, P.D. Adams, G.M. Clore, W.L. DeLano, P. Gros, R.W. Grosse-Kunstleve, J.S. Jiang, J. Kuszewski, M. Nilges, N.S. Pannu, R.J. Read, L.M. Rice, T. Simonson, G.L. Warren, Crystallography and NMR system: a new software suite for macromolecular structure determination, Acta Cryst. D 54 (1998) 905–921.

[18] A.T. Brunger, Free *R* value: a novel statistical quantity for assessing the accuracy of crystal structures, Nature 355 (1992) 472–475.

[19] H. Pan, X.L. Liu, L.L. Ou-Yang, G.Z. Yang, Y.C. Zhou, Z.P. Li, X.F. Wu, Diversity of cDNAs encoding phospholipase A_2 from *Agkistrodon halys* Pallas venom, and its expression in *E. coli*, Toxicon 36 (1998) 1155–1163.

[20] R. Laskowski, M. Macarthur, D. Moss, J. Thornton, Procheck: a program to check stereochemical quality of protein structures, J. Appl. Cryst. 26 (1993) 283–290.

[21] M.M. Teeter, Water structure of a hydrophobic protein at atomic resolution: pentagon rings of water molecules in crystals of crambin, Proc. Natl. Acad. Sci. USA 81 (1984) 6014–6018.

[22] R.K. Arni, R.J. Ward, Phospholipase A_2—a structural review, Toxicon 34 (1996) 827–841.

[23] N.C.J. Strynadka, M.N.G. James, Crystal structures of the helix–loop–helix calcium-binding proteins, Ann. Rev. Biochem. 58 (1989) 951–998.

[24] S.P. White, D.L. Scott, Z. Otwinowski, M.H. Gelb, P.B. Sigler, Crystal structure of cobra venom phospholipase A_2 in a complex with a transition state analogue, Science 250 (1990) 1560–1563.
[25] J.H. Naismith, J. Habash, S.J. Harrop, J.R. Helliwell, W.N. Hunter, T.C.M. Wan, S.J. Weisgerber, A.J. Kalb (Gilboa), J. Yariv, Refined structure of cadmium substituted concanavalin A at 2.0 Å resolution, Acta Cryst. D49 (1993) 561–571.
[26] N. Yao, S. Trakhanov, F.A. Quiocho, Refined 1.89 Å structure of the histidine-binding protein complexed with histidine and its relationship with many other active transport/chemosensoproteins proteins, Biochemistry 33 (1994) 4769–4779.
[27] N.O. Concha, B.A. Rasmussen, K. Bush, O. Herzberg, Crystal structures of the cadmium- and mercury-substituted metallo-β-lactamase from *Bacteroides fragilis*, Protein Sci. 6 (1997) 2671–2676.
[28] S. Trakhanov, D.I. Kreimer, S. Parkin, G.F. Ames, B. Rupp, Cadmium-induced crystallization of proteins: II. Crystallization of the *Salmonella typhimurium* histidine-binding protein in complex with L-histidine, L-arginine, or L-lysine, Protein Sci. 7 (1998) 600–604.
[29] D.L. Scott, S.P. White, Z. Otwinowski, W. Yuan, M.H. Gelb, P.B. Sigler, Interfacial catalysis: the mechanism of phospholipase A_2, Science 250 (1990) 1541–1546.
[30] R.A. Steiner, H.J. Rozeboom, A. De Vries, K.H. Kalk, G.N. Murshudov, K.S. Wilson, B.W. Dijkstra, X-ray structure of bovine pancreatic phospholipase A_2 at atomic resolution, Acta Cryst. D57 (2001) 516–526.
[31] B.C. Finzel, P.C. Weber, D.H. Ohlendorf, F.R. Salemme, Crystallographic refinement of bovine pro-phospholipase A_2 at 1.6 Å resolution, Acta Cryst. B47 (1991) 814–816.
[32] P.J. Kraulis, MOLSCRIPT: a program to produce both detailed and schematic plots of protein structures, J. Appl. Cryst. 24 (1991) 946–950.
[33] E.A. Merritt, D.J. Bacon, Raster3D: photorealistic molecular graphics, Method Enzymol. 277 (1997) 505–524.